**Wind and Structures**, *Vol. 27, No. 3 (2018) 149-161*
DOI: https://doi.org/10.12989/was.2018.27.3.149


# Flutter reliability analysis of suspension bridges based on multiplicative dimensional reduction method

Junfeng Guo[1], Shixiong Zheng[*1], Jin Zhang[1], Jinbo Zhu[1] and Longqi Zhang[2]

[1]*School of Civil Engineering, Southwest Jiaotong University, Chengdu, China, 610031*
[2]*Department of road and bridge engineering, Sichuan Vocational and Technical College of Communications, Chengdu, China, 611130*

*(Received August 10, 2017, Revised February 22, 2018, Accepted March 15, 2018)*

**Abstract.** A reliability analysis method is proposed in this paper based on the maximum entropy (MaxEnt) principle in which constraints are specified in terms of the fractional moments instead of integer moments. Then a multiplicative dimensional reduction method (M-DRM) is introduced to compute the fractional moments. The method is applicable for both explicit and implicit limit state functions of complex structures. After two examples illustrate the accuracy and efficiency of this method in comparison to the Monte Carlo simulation (MCS), the method is used to analyze the flutter reliability of suspension bridge. The results show that the empirical formula method in which the limit state function is explicitly represented as a function of variables is only a too conservative estimate for flutter reliability analysis but is not accurate adequately. So it is not suitable for reliability analysis of bridge flutter. The actual flutter reliability analysis should be conducted based on a finite element method in which limit state function is implicitly represented as a function of variables. The proposed M-DRM provide an alternate and efficient way to analyze a much more complicated flutter reliability of long span suspension bridge.

**Keywords:** reliability analysis; failure probability; flutter; multiplicative dimensional reduction method (M-DRM); principle of maximum entropy

## 1. Introduction

Recently, as the span of suspension bridge is longer and longer, it is more and more sensitive to wind. Thus, the flutter analysis of this kind of bridges has been the subject of many researches (Larsen 1997, Agar 1988, Chen and Cai 2003, Han *et al*. 2015, Zhang *et al.* 2011). These studies were conducted based on an assumption that all the parameters of bridge are complete deterministic. Researchers usually call this deterministic flutter analysis. In reality, however, there are many uncertainties during the process of erection of the bridge. The parameters of bridge may fluctuate in the vicinity of the nominal values rather than be exactly equal to them. These uncertainties include material mechanical properties, geometric properties and wind characteristics, etc. Compared with flutter reliability analysis, the deterministic analysis can't provide complete and accurate information adequately. Therefore, the flutter analysis should be studied from a probabilistic perspective (Milev and Tagliani 2017, Gzyl *et al*. 2017, Zhang and Pandey 2013, Zhang *et al*. 2011, Pandey and Zhang 2012, Shi *et al*. 2016).

Unlike the deterministic flutter analysis of suspension bridges, the probabilistic flutter analysis has not been well studied. Considering the uncertainties of wind load parameters, Prenninger *et al*. (1990) studied the reliability of two kinds of long span bridges respectively-a cable stayed and a suspension bridge. Ostenfeldrosenthal *et al.* (1992) studied the flutter reliability of cable-supported bridges by considering several variables including structural damping, turbulence intensity, extreme wind speeds and conversion of results from model tests to prototype bridges. Ge *et al*. (2000) proposed a reliability analysis model based on first order reliability method (FORM) to study the flutter reliability of bridge. According to the fundamental theory of reliability, Pourzeynail and Datta (2002) calculated the flutter failure probability of suspension bridge. In these studies above, the limit state function is considered to be explicit formula. In other words, the flutter reliability analysis is conducted based on empirical formula. The uncertainties included in wind loads and resistances are simply considered in explicit limit state function based on some assumptions.

However, in fact, the flutter response of bridges should be calculated by an implicit function. That is to say, a closed empirical formula solution of flutter response can't consider the complexity of structure and the diversity of random variables. Therefore, the basic theory of reliability, first order reliability method (FORM) and second order reliability method (SORM) used in previous studies are not suitable any more.

Monte Carlo simulation (MCS) is a traditional method for reliability analysis of structures. This method is not only simple and easy to conduct but also suitable for both explicit and implicit limit state function. Thus, the method is often regarded as a standard to validate the analysis results of other methods. However, computation efficiency

*Corresponding author, Professor
E-mail: zhengsx@home.swjtu.edu.cn



ISSN: 1226-6116 (Print), 1598-6225 (Online)

of the method is very low for complicated structure. So the method is obviously not appropriate for complicated flutter analysis.

Response surface method (RSM) is an available method for reliability analysis of implicit limit state functions. The main idea of this method is to replace the complex implicit limit state function by a simple response surface function. A major advantage of RSM is that implicit limit state function can be transformed to explicit form (Bucher and Bourgund 1990, Rajashekhar and Ellingwood 1993, Faravelli 1989, Yao and Wen 1996, Huh and Haldar 2001, Kaymaz and McMahon 2005). Some scholars have studied the reliability of structure based on RSM. Liu and Moses (1994) improved the RSM based on Monte Carlo importance sampling (RSM-MCIS) to study the structural reliability. Huh and Haldar (2002) used systematic RSM to study the seismic reliability of nonlinear frames. Zheng and Das (2000) improved the RSM and then applied it to stiffened plate reliability analysis. However, RSM has also unavoidable shortcomings for structural reliability analysis. The general response surface function of the structure is usually established only in local definition domain and the approximation accuracy of the response surface function is rapidly deteriorated in other domains. So when the structural design parameters change, continuous experiment redesign and reestablishing of the response surface is unavoidable (Zhang *et al*. 2011). On the other hand, the RSM-MCIS may produce significant errors due to the noise added in limit state function obtained by RSM (Cheng *et al*. 2005). Thus, an alternative reliability method which is accurate, efficient, and appreciate for both explicit and implicit limit state functions is required.

The principle of maximum entropy (MaxEnt) proposed by Jaynes (1957) is another method for reliability analysis. Interest in MaxEnt principle has raised with the emergence of concept of fractional moments (Inverardi *et al.* 2005, Taufer *et al.* 2009, Milev *et al*. 2012).Some scholars have developed the method with fractional moments. Zhang and Pandey (2013) studied structural reliability based on the concepts of entropy, fractional moment and dimensional reduction method. Balomenos *et al.* (2015) conducted reliability analysis of reinforced concrete slabs by dimensional reduction method. Based on previous studies, the purpose of this paper is to propose a more robust and efficient method for probabilistic finite element analysis with application to flutter of suspension bridges. The proposed method is multiplicative dimensional reduction method (M-DRM), which provides a highly accurate approximation of the response distribution. The basic procedures of proposed method are (1) Obtaining the explicit or implicit limit state function. (2) Computing the parameters of MaxEnt distribution based on M-DRM. (3) Using the obtained parameters to get probability density function (PDF), then calculate the failure probability of structure. After two numerical examples are discussed in this paper to demonstrate the efficiency and accurate of the method, the flutter reliability analysis of suspension bridge is conducted based on M-DRM.

## 2. Multiplicative dimensional reduction method

### *2.1 Evaluation of the response statistical moments*

The structural reliability response can be calculated by a function of some input variables. For instance, when the capacity of a reinforced concrete beam is evaluated, one output variable of interest is the ultimate bending moment. This can be described by a function of some input variables, such as width of beam, area of reinforcement, yield stress of reinforcement, etc., which is denoted as

$$Y = h\left(\bar{X}\right) \tag{1}$$

Where Y is a scalar of output response and $\bar{X}$ is a vector of input random variables, i.e. $\bar{X} = X_1, X_2, ..., X_n$.

The probability of a structural failure due to Y less than a certain value can be obtained after knowing the probability distribution of all random variables $\bar{X}$, which can be denoted as

$$p_f = p\left[h\left(\bar{X}\right) - y_c \le 0\right] \tag{2}$$

Where $p_f$ is the probability of a structural failure and $y_c$ is a certain value, where each output response less than this certain value leads to structural failure.

So the limit state function can be defined as

$$g\left(\bar{X}\right) = h\left(\bar{X}\right) - y_c \tag{3}$$

The probability of failure can be calculate by the following integral

$$p_f = \int_{[g(\bar{X})\le 0]} f_{\bar{x}}(\bar{x})d\bar{x} \tag{4}$$

Where $[g(\bar{X})\le 0]$ represents the failure domain and $f_{\bar{x}}(\bar{x})$ is the reinforced concrete beam probability density function (PDF) of the previous defined vector $\bar{X}$.

According to Balomenos (2015), the integral can be calculated usually by using three methods: (1) Direct integration, but the PDF is hardly available when limit state function is implicit and the dimension of integral is usually too large to calculate conveniently; (2) Simulations, such as Monte Carlo simulation (MCS), but the efficiency of calculation about it is very low. Especially when the number of uncertain parameters is more, this method always costs much computational time; (3) Approximate methods, such as first- and second- order reliability methods (FORM and SORM), but they also can't consider the implicit limit state function. And they can give accurate solutions only for extremely large failure probability problems (Cheng *et al*. 2005).

Li and Zhang (2011) thought that the method of moment is another way for calculating structural reliability since it costs much less computational time and requires no iterations. Comprehensively analyzing all kinds of the methods of moment such as additive dimensional reduction method (A-DRM), high-dimensional model representation (H-DRM) and M-DRM, Balomenos (2015) in his Ph.D. thesis point out that only the M-DRM principle can be adopted since it makes the computation of both fractional

and integer moments of response easy and simple.

According to the proposed A-DRM method in previous studies (Rabitz and Alis 1999, Li *et al.* 2001, Rahman and Xu 2004), a scalar of output response have the following approximate form

$$Y = h(\bar{X}) \approx h_1(X_1) + h_2(X_2) + ... + h_n(X_n) - (n-1)h_0 = \sum_{i=1}^{n} h_i(X_i) - (n-1)h_0 \quad (5)$$

Where $h_0$ defines the output response when all of the random variables are fixed to the mean values, i.e., $h_0 = h(c_1, c_2, ..., c_n) =$ a constant, $h_i(X_i)$ is an one-dimensional cut function, i.e., $h_i(X_i) = h(c_1, c_2, ..., X_i, ..., c_n)$ and $c_1, c_2, ..., c_n$ corresponds to the mean value of each random variables.

Unlike the A-DRM, the response function can be transformed logarithmically by M-DRM method, which can derive the multiplicative approximation of the response function as

$$Y = h(\bar{X}) \approx h_0^{(1-n)} \times [h_1(X_1) \times h_2(X_2) \times ... \times h_n(X_n)] = h_0^{(1-n)} \times \prod_{i=1}^{n} h_i(X_i) \quad (6)$$

Thus, according to the M-DRM, a scalar function Eq. (5) can be replaced by a product form Eq. (6). The product form makes both integer and fractional moments of response easy to get.

According to the M-DRM representation above, a k[th] statistical moment of the response function Eq. (6) can be written as

$$E[Y^k] = E[(h(\bar{X}))^k] \approx E[(h_0^{(1-n)} \times \prod_{i=1}^{n} h_i(X_i))^k] \quad (7)$$

Where the mathematical expectation operation is denoted as E [ ] and when k=1, E [ $Y^k$ ] = E [Y] represents the expected value of Y, i.e., the mean value of Y.

Based on a basic assumption that all input random variables are exactly independent, Eq. (7) can be rewritten as

$$\begin{aligned} E[Y^k] &\approx \left(h_0^{(1-n)}\right)^k \times E\left[\left(h_1(X_1)\right)^k\right] \times E\left[\left(h_2(X_2)\right)^k\right] \times ... \times E\left[\left(h_n(X_n)\right)^k\right] \\ &= h_0^{k(1-n)} \prod_{i=1}^{n} E\left[\left(h_i(X_i)\right)^k\right] \end{aligned} \quad (8)$$

The evaluation of a k[th] statistical moment of output response Y need the calculation of the k[th] moments of all the cut functions though one-dimensional integration.

$$E\left[(h_i(X_i))^k\right] = \int_{x_i} [h_i(x_i)]^k f_i(x_i) dx_i \quad (9)$$

For simplicity, the numerical integration of Gauss quadrature formulas can be used instead of one-dimensional integration. For example, a k[th] moment of an i[th] cut function can be approximated as a weighted sum

$$\int_{x_i} [h(x_i)]^k f_i(x_i) dx_i \approx \sum_{j=1}^{L} w_j [h_i(z_j)]^k \quad (10)$$

Where L is the number of the Gauss quadrature points, $w_j$ and $z_j$ are the weights and coordinates of the Gauss quadrature points (j=1,…, L) and $h_i(z_j)$ (i=1,2…,n; j=1,…,L) is the structural response when $i^{th}$ cut function is set at $j^{th}$ Gauss quadrature point.

Table 1 lists the Gaussian integration schemes which was derived for Normal, Lognormal and Gumbel. Table 2 lists the Gauss Weights ( $w_j$ ) and Gauss Points ( $z_j$ ) of the five-order rule ($L$=5) of Gauss-Laguerre quadratures, Gauss-Hermite, Gauss-Legendre schemes. For more orders of Gauss Weights ( $w_j$ ) and Gauss points ( $z_j$ ), one can refer to the literature for details (Davis and Rabinowitz 1984, Zwillinger 2011, Hong *et al*. 2015)

### *2.2 Response function probability distribution using maximum entropy method*

MaxEnt optimization procedure can be conducted with integer moments or fractional moments respectively. Ramirez and Carta (2006) used MaxEnt optimization procedure with integer moments constraints to derive the wind probability distribution, but Pandey and Zhang (2012)

Table 1 Gaussian integration of formula for one-dimension fractional moment calculation

| Distribution | Support domain | Gaussian Quadrature | Numerical integration Formula |
|---|---|---|---|
| Normal | $(-\infty, +\infty)$ | Gauss-Hermite | $\sum_{j=1}^{L} w_j [h(u + \sigma z_j)]^k$ |
| Lognormal | $(0, +\infty)$ | Gauss-Hermite | $\sum_{j=1}^{L} w_j \{h[\exp(\tilde{u} + \tilde{\sigma} z_j)]\}^k$ |
| Gumbel | $(0, +\infty)$ | Gauss-Laguerre | $\sum_{j=1}^{L} w_j [h(-\frac{1}{a}\ln z_j + u)]^k$ |

Note: $\tilde{\sigma} = \ln[1 + \frac{\sigma}{u}], \tilde{u} = \ln(u) - \frac{1}{2}\tilde{\sigma}^2$

Table 2 Weights and points of five-order Gaussian quadrature rules

| Gaussian rules | L | 1 | 2 | 3 | 4 | 5 |
|---|---|---|---|---|---|---|
| Gauss-Legendre | $w_j$ | 0.23693 | 0.47863 | 0.56889 | 0.47863 | 0.23693 |
| | $z_j$ | -0.90618 | -0.53847 | 0 | 0.53847 | 0.90618 |
| Gauss-Hermite | $w_j$ | 0.01126 | 0.22208 | 0.53333 | 0.22208 | 0.01126 |
| | $z_j$ | -2.85697 | -1.35563 | 0 | 1.35563 | 2.85697 |
| Gauss-Laguerre | $w_j$ | 0.52176 | 0.39867 | 0.07594 | 0.00361 | 0.00002 |
| | $z_j$ | 0.26356 | 1.4134 | 3.5964 | 7.0858 | 12.641 |

studied the reliability analysis of the robotic manipulator and point that the estimation error would increase as the order of the integer moments increases. Furthermore, a few fractional moments are far more effective in summarizing the entire distribution than integer moments (Zhang and Pandey 2013).

So the Eqs. (8) and (10) can be rewritten as

$$E[Y^{\alpha}] \approx h_0^{\alpha(1-n)} \prod_{i=1}^{n} E\left[\left(h_i\left(X_i\right)\right)^{\alpha}\right] \tag{11}$$

$$E[(h_i(X_i))^{\alpha}] \approx \sum_{j=1}^{L} w_j [h_i(z_j)]^{\alpha} \tag{12}$$

Where $\alpha$ is a fraction.

After getting the response statistical moments, the most unbiased probability distribution of response can be estimated by MaxEnt principle with fractional moments. The true entropy of response variable Y can be written as

$$H[f] = -\int_Y f_Y(y) In[f_Y(y)] dy \tag{13}$$

Where, $f_Y(y)$ is the probability density function of response variable Y.

The Lagrangian function associated with the MaxEnt problem is written as

$$\begin{aligned} &L[\lambda, \alpha; f_Y(y)] = -\int_Y f_Y(y) In[f_Y(y)] dy - (\lambda_0 - 1)[\int_Y f_Y(y) dy - 1] \\ &-\sum_{i=1}^{m} \lambda_i [\int_Y y^{\alpha_i} f_Y(y) dy - M_Y^{\alpha_i}] \end{aligned} \tag{14}$$

Where $\lambda = [\lambda_0, \lambda_1, ..., \lambda_m]^T$ are the Lagrange multipliers; $\alpha = [\alpha_1, ..., \alpha_m]^T$ are the fractions associated with the fractional moments; $M_Y^{\alpha_i}$ represents the i$^{th}$ fractional moment of response variable Y; m is the number of fractional moments.

For optimal solution, Eq. (14) must meet a key condition as follow

$$\frac{\partial L[\lambda, \alpha; f_Y(y)]}{\partial f_Y(y)} = 0 \tag{15}$$

When $i$=0, $\alpha_0$=0. Thus, we can obtain the estimated PDF ( $\tilde{f}_Y(y)$ ) of true PDF ( $f_Y(y)$ ) from the Eq. (15)

$$\tilde{f}_Y(y) = \exp(-\sum_{i=0}^{m} \lambda_i y^{\alpha_i}) \tag{16}$$

According to the principle of the normalization condition that the integration of the PDF must be exactly equal to 1, $\lambda_0$ can be defined as follow

$$\lambda_0 = \ln[\int_Y \exp(-\sum_{i=1}^{m} \lambda_i y^{\alpha_i}) dy] \tag{17}$$

A significant advantage of the proposed computational approach is that the fractions $\alpha_i$ ($i$=1, 2,…,m) do not need to be specified a priori, since they can be calculated as a part of the entropy maximization procedure (Balomenos 2015). In order to achieve the idea of the MaxEnt optimization with fractional moments, the cross-entropy which represents the minimization of the Kullback-Leibler (K-L) divergence between the estimated PDF ( $\tilde{f}_Y(y)$ ) and the true PDF ( $f_Y(y)$ ) is used here

$$\begin{aligned} &K[f, \tilde{f}] = \int_Y f_Y(y) \ln[f_Y(y) / \tilde{f}_Y(y)] dy = \\ &\int_Y f_Y(y) \ln[f_Y(y)] dy - \int_Y f_Y(y) \ln[\tilde{f}_Y(y)] dy \end{aligned} \tag{18}$$

Substituting $\tilde{f}_Y(Y)$ from Eq. (16) and $H[f]$ from Eq. (13) into Eq. (18) and taking into account Eq. (11), the K-L divergence can be rewritten as

$$K[f, \tilde{f}] = -H[f] + \lambda_0 + \sum_{i=1}^{m} \lambda_i M_Y^{\alpha_i} \tag{19}$$

Where $H[f]$ is the entropy of the true PDF which is independent of $\lambda$ and $\alpha$. Therefore, minimization of the K-L divergence implies the following function minimization

$$I(\lambda, \alpha) = K[f, \tilde{f}] + H[f] = \lambda_0 + \sum_{i=1}^{m} \lambda_i M_Y^{\alpha_i} \tag{20}$$

Therefore, MaxEnt parameters with fractional moments, i.e., the fractional exponents ($\alpha_i$) and the Lagrange multipliers ( $\lambda_i$ ) can be obtained by using the following optimization

$$\begin{cases} Find: \{\alpha_i\}_{i=1}^{m} \{\lambda_i\}_{i=1}^{m} \\ Minimize: I(\lambda, \alpha) = \ln[\int_Y \exp(-\sum_{i=1}^{m} \lambda_i y^{\alpha_i}) dy] + \sum_{i=1}^{m} \lambda_i M_Y^{\alpha_i} \end{cases} \tag{21}$$

The Eq. (21) can be conducted in MATLAB with the simplex search method (Lagarias *et al*. 1998). Substituting these obtained parameters into Eq. (16), then we can get the estimated PDF of output response.

### *2.3 Procedure for the proposed method*

The procedures of the proposed method are:

(1) Obtaining the limit state function (explicit or implicit) of output response;

(2) Evaluation of the response statistical moments;

(3) Calculation of response probability density function (PDF) by M-DRM method;

(4) Calculation of failure probability of structure by PDF.

A flow chart for the M-DRM method with fractional moments is given in Fig. 1.

## 3. Verification examples and investigations

Because a direct verification of the complicated suspension bridge flutter is very difficult, two relative simple examples are presented here to investigate the computation efficiency and accuracy of the M-DRM method for reliability analysis. The first example is a simply supported beam. This example demonstrates the accuracy and efficiency of M-DRM method for reliability analysis by comparison with other methods such as FORM and SORM.

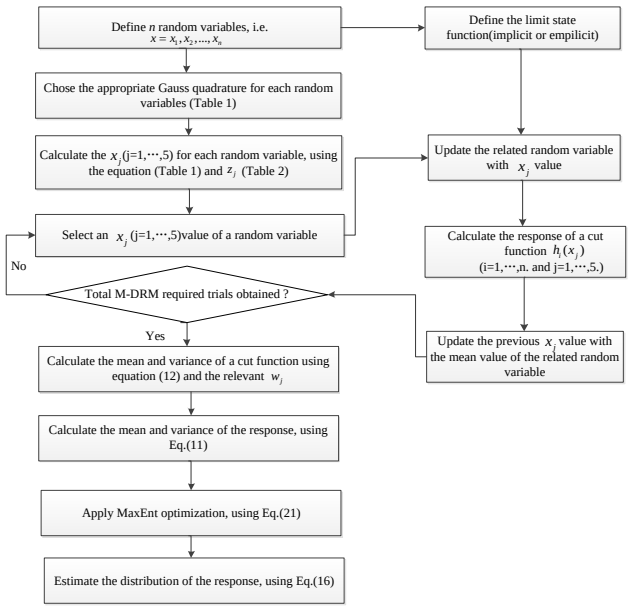


Fig. 1 Flow chart for the procedures of the M-DRM method

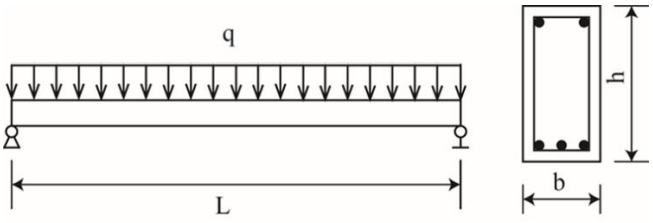


Fig. 2 The simply supported beam

The second example is a linear frame structure. This example demonstrates the application where the limit state function is not available, i.e., the limit state function is implicit.

### *3.1 Example 1: Simply supported beam (explicit limit state function)*

Considering a concrete beam shown in Fig. 2, the ultimate bending moment of resistance $M_U$ and ultimate shearing force of resistance $V_U$ are given by explicit functions, respectively.

The ultimate bending moment of resistance $M_U$

$$M_U = f_y A_s (h_0 - \frac{1}{2}\frac{f_y A_s}{f_c b}) \tag{22}$$

The ultimate shearing force of resistance $V_U$

$$V_U = 0.663 f_t b h_0 + f_{yv}\frac{A_{sv}}{s} h_0 + 0.015 f_c b h_0 \tag{23}$$

Where $f_y$ is yield strength of steel bar; $f_{yv}$ is yield strength of web reinforcement; $f_c$ is compressive strength of concrete; $f_t$ is tensile strength of concrete; $h$ is depth of cross section, $h_0 = h - 0.035m$; $b$ is width of cross section; As is area of reinforced bars; Asv is area of web reinforcement; $s$ is the spacing of web reinforcement, $s$=150mm; strength level of concrete = C25.

Thus, the limit state functions of the ultimate bending moment of resistance and ultimate shearing force of resistance for reliability analysis are defined as

$$\begin{cases} g_M = M_U - M_B \\ g_V = V_U - V_B \end{cases} \tag{24}$$

Where $M_B$ is maximum bending moment exerted in the beam; $V_B$ is maximum shearing force exerted in the beam. $q = 40kN/m$, $L$= 3.6m, $M_B = \frac{1}{8}qL^2$, $V_B = \frac{1}{2}qL$.

From the Eq. (24), one can see that the failure probabilities of the ultimate bending moment and shearing force can be computed as $P_F = P_r[g_M \le 0]$ and $P_F = P_r[g_V \le 0]$, respectively.

Considering five input random variables of structure, their distributions are listed in Table 3.

Firstly, four integer product moments of bending moment resistance and shearing force resistance are computed using M-DRM and MCS methods, respectively. Numerical moment integration grid based on Gaussian rules is given in Table 4 and the integration points of each variable are highlighted. Method proposed in section 2.1 is used to determine the integration gird, which can help reader to verify the numerical results. It is worth noting that the calculations of MaxEnt distribution and statistical moment are only based on the 26 (=1+5×5) deterministic model evaluations.

Numerical accuracy of four integer moments obtained from M-DRM is compared against the benchmark results obtained from MCS with $10^6$ samples. Results from the Table 5 show that M-DRM estimates have less than 0.1% error for all the four integer moments of both bending moment resistance and shearing force resistance.

As shown in Fig. 3, the estimated PDFs of the ultimate bending moment $M_U$ and shearing force $V_U$, obtained from M-DRM proposed in section 2 are in consistent with those obtained from the MCS method. The Lagrangian multipliers and the fractional moments of the estimated MaxEnt PDFs obtained from M-DRM are listed in Tables 6 and 7.

Considering the limit state functions Eq. (24), then the probabilities of failure can be computed by FORM, SORM, M-DRM and MCS methods respectively, and the results are listed in Table 8.

Table 3 Random variables in the simply supported beam example

| Variable | Distribution | Mean | Units | Cov | Reference |
|---|---|---|---|---|---|
| $f_y$ | Normal | 3.50E8 | Pa | 0.05 | Nowak et al.2003 |
| $f_{yv}$ | Normal | 3.00E8 | Pa | 0.05 | |
| $f_c$ | Normal | 1.67E7 | Pa | 0.15 | |
| $h$ | Gumbel | 0.40 | m | 0.1 | Assumed |
| $b$ | Gumbel | 0.20 | m | 0.1 | |

Table 4 Numerical integration grid for computing the moments with M-DRM: simply supported beam example

| Variable | NO. | Numerical integration grid | | | | | $M_U$ ($KN \cdot m$) | $V_U$ ($KN$) |
|---|---|---|---|---|---|---|---|---|
| | | $f_y$ (Pa) | $f_{yv}$ (Pa) | $f_c$ (Pa) | $h$ (m) | $b$ (m) | | |
| $f_y$ | 1 | **3.000E+08** | 3.000E+08 | 1.670E+07 | 0.4 | 0.2 | 75.741 | 145.717 |
| | 2 | **3.263E+08** | 3.000E+08 | 1.670E+07 | 0.4 | 0.2 | 81.626 | 145.717 |
| | 3 | **3.500E+08** | 3.000E+08 | 1.670E+07 | 0.4 | 0.2 | 86.837 | 145.717 |
| | 4 | **3.737E+08** | 3.000E+08 | 1.670E+07 | 0.4 | 0.2 | 91.950 | 145.717 |
| | 5 | **4.000E+08** | 3.000E+08 | 1.670E+07 | 0.4 | 0.2 | 97.497 | 145.717 |
| $f_{yv}$ | 6 | 3.500E+08 | **2.571E+08** | 1.670E+07 | 0.4 | 0.2 | 86.837 | 139.820 |
| | 7 | 3.500E+08 | **2.797E+08** | 1.670E+07 | 0.4 | 0.2 | 86.837 | 142.919 |
| | 8 | 3.500E+08 | **3.000E+08** | 1.670E+07 | 0.4 | 0.2 | 86.837 | 145.717 |
| | 9 | 3.500E+08 | **3.203E+08** | 1.670E+07 | 0.4 | 0.2 | 86.837 | 148.515 |
| | 10 | 3.500E+08 | **3.429E+08** | 1.670E+07 | 0.4 | 0.2 | 86.837 | 151.614 |
| $f_c$ | 11 | 3.500E+08 | 3.000E+08 | **9.558E+06** | 0.4 | 0.2 | 78.851 | 137.896 |
| | 12 | 3.500E+08 | 3.000E+08 | **1.331E+07** | 0.4 | 0.2 | 84.116 | 142.006 |
| | 13 | 3.500E+08 | 3.000E+08 | **1.670E+07** | 0.4 | 0.2 | 86.837 | 145.717 |
| | 14 | 3.500E+08 | 3.000E+08 | **2.009E+07** | 0.4 | 0.2 | 88.640 | 149.428 |
| | 15 | 3.500E+08 | 3.000E+08 | **2.384E+07** | 0.4 | 0.2 | 90.039 | 153.538 |
| $h$ | 16 | 3.500E+08 | 3.000E+08 | 1.670E+07 | **0.4236** | 0.2 | 93.142 | 155.138 |
| | 17 | 3.500E+08 | 3.000E+08 | 1.670E+07 | **0.3712** | 0.2 | 79.140 | 134.217 |
| | 18 | 3.500E+08 | 3.000E+08 | 1.670E+07 | **0.3421** | 0.2 | 71.354 | 122.582 |
| | 19 | 3.500E+08 | 3.000E+08 | 1.670E+07 | **0.3209** | 0.2 | 65.700 | 114.134 |
| | 20 | 3.500E+08 | 3.000E+08 | 1.670E+07 | **0.3028** | 0.2 | 60.874 | 106.923 |
| $b$ | 21 | 3.500E+08 | 3.000E+08 | 1.670E+07 | 0.4 | **0.2118** | 87.433 | 151.879 |
| | 22 | 3.500E+08 | 3.000E+08 | 1.670E+07 | 0.4 | **0.1856** | 86.008 | 138.196 |
| | 23 | 3.500E+08 | 3.000E+08 | 1.670E+07 | 0.4 | **0.1710** | 85.027 | 130.587 |
| | 24 | 3.500E+08 | 3.000E+08 | 1.670E+07 | 0.4 | **0.1604** | 84.202 | 125.062 |
| | 25 | 3.500E+08 | 3.000E+08 | 1.670E+07 | 0.4 | **0.1514** | 83.408 | 120.346 |
| Mean-value | 26 | 3.500E+08 | 3.000E+08 | 1.670E+07 | 0.4 | 0.2 | 86.837 | 145.717 |

Table 5 Integer moments of the ultimate bending moment and shearing force

| Method | Moments ($M_U$) | | | | Moments ($V_U$) | | | |
|---|---|---|---|---|---|---|---|---|
| | 1st | 2nd | 3rd | 4th | 1st | 2nd | 3rd | 4th |
| M-DRM | 86.450 | 7605 | 6.8040E+5 | 6.1870E+7 | 145.73 | 2.1612E+4 | 3.2605E+6 | 5.0018E+8 |
| MCS | 86.451 | 7606.9 | 6.8079E+5 | 6.1928E+7 | 145.72 | 2.1610e+04 | 3.2600e+06 | 5.0005e+08 |
| Relative error(%) | -1E-3 | -2.4E-2 | -5.7E-2 | -9.4E-2 | 6.8E-3 | 9.3E-3 | 1.5E-2 | 2.6E-2 |

Table 6 Parameters of MaxEnt PDF of $M_U$ derived from M-DRM

| Entropy | $m$ | 0 | 1 | 2 | 3 |
|---|---|---|---|---|---|
| 3.8815 | $\lambda_m$ | 28.3333 | -1.4620 | 0.6548 | 1.7483 |
| | $\alpha_m$ | | 1.2402 | 1.3867 | 0.6088 |
| | $M_Y^{\alpha_m}$ | | 252.9409 | 487.1855 | 15.0721 |

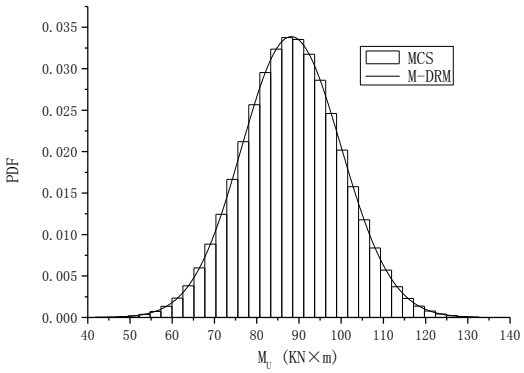


(a) $M_U$

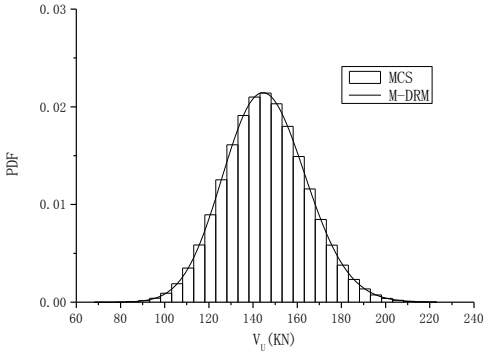


(b) $V_U$

Fig. 3 Distributions of the ultimate bending moment and shearing force

Table 7 Parameters of MaxEnt PDF of $V_U$ derived from M-DRM

| Entropy | $m$ | 0 | 1 | 2 | 3 |
|---|---|---|---|---|---|
| | $\lambda_m$ | 73.7373 | -1.2616 | 1.2490 | -4.3845 |
| 4.365405 | $\alpha_m$ | | 0.5456 | 1.0649 | 0.8497 |
| | $M_Y^{\alpha_m}$ | | 15.1205 | 201.4566 | 68.8568 |

Table 8 Results of example 1

| Method | Ultimate bending moment ($M_U$) | | Ultimate shearing force ($V_U$) | |
|---|---|---|---|---|
| | $P_f$ | Relative error (%) | $P_f$ | Relative error (%) |
| FORM | 0.0248 | 11 | 6.18E-6 | 23.6 |
| SORM | 0.0267 | 4.3 | 5.81E-6 | 16.2 |
| M-DRM | 0.0277 | 0.72 | 4.94E-6 | 1.2 |
| MCS | 0.0279 | - | 5E-6 | - |

From the Table 8, one can see that the results obtained from M-DRM method agree more well with the exact results obtained from MCS method than other methods (FORM, SORM). In other words, the relative error of M-DRM is the smallest. Furthermore, the M-DRM method is more efficiency of calculation than MCS. This is because that the calculations of MaxEnt distribution and statistical moment are only based on the 26 (=1+5 × 5) deterministic model evaluations, but MCS is based on $10^6$ samples.

### *3.2 Example 2: Linear frame structure (implicit limit state function)*

The second example discussed here is a linear frame structure as shown in Fig. 4. Different horizontal loads $P_i$ ($i$=1, 2), cross sectional area $A$ and the Young's modulus $E$ are treated as exactly independent random variables. These input random variables and their distributions are listed in Table 9. The sectional moment of inertia is expressed as $I = \alpha A^2 (\alpha = 0.08333)$. The focus of concern here is the probability that the horizontal displacement at node 3 exceeds 0.015 m. Thus, the limit state function can be expressed as

$$g(E, A, P_1, P_2) = 0.015 - u_3(E, A, P_1, P_2) \tag{25}$$

In this example, FORM and SORM methods are not appropriate any more since the limit state function is implicit in terms of input random variables. So we can use M-DRM and MCS to calculate the probability of failure respectively below.

Using the five Gaussian points of Table 2 to calculate the integration of each component function. Then the entire numerical integration grid can be obtained and the results are listed in Table 10, in which one can see that the totally number of deterministic model evaluation is only 21(=1+4 × 5).

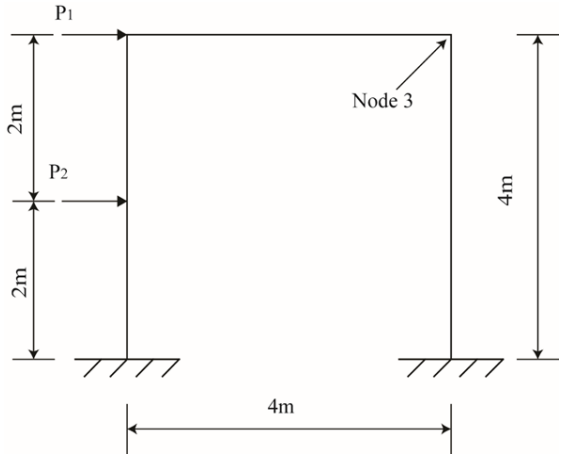


Fig. 4 Linear portal frame

Table 9 Random variables in the linear frame structure

| Variable | Distribution | Mean | Units | Cov | Reference |
|---|---|---|---|---|---|
| E | Normal | 2.1e11 | Pa | 0.1 | Zhang and Pandey 2013 |
| A | Lognormal | 0.04 | $m^2$ | 0.1 | |
| $P_1$ | Lognormal | 50000 | N | 0.1 | |
| $P_2$ | Lognormal | 20000 | N | 0.1 | |

Table 10 Numerical integration grid for computing the moments with M-DRM: Linear frame structure example

| Variable | NO. | Numerical integration grid | | | | Horizontal displacement at node 3（mm） |
|---|---|---|---|---|---|---|
| | | E(Pa) | A($m^2$) | $P_1$(N) | $P_2$(N) | |
| E | 1 | **1.500E+11** | 4.000E-02 | 5.000E+04 | 2.000E+04 | 15.324 |
| | 2 | **1.815E+11** | 4.000E-02 | 5.000E+04 | 2.000E+04 | 12.664 |
| | 3 | **2.100E+11** | 4.000E-02 | 5.000E+04 | 2.000E+04 | 10.945 |
| | 4 | **2.385E+11** | 4.000E-02 | 5.000E+04 | 2.000E+04 | 9.637 |
| | 5 | **2.700E+11** | 4.000E-02 | 5.000E+04 | 2.000E+04 | 8.513 |
| A | 6 | 2.100E+11 | **3.033E-02** | 5.000E+04 | 2.000E+04 | 19.040 |
| | 7 | 2.100E+11 | **3.499E-02** | 5.000E+04 | 2.000E+04 | 14.305 |
| | 8 | 2.100E+11 | **3.982E-02** | 5.000E+04 | 2.000E+04 | 11.045 |
| | 9 | 2.100E+11 | **4.531E-02** | 5.000E+04 | 2.000E+04 | 8.530 |
| | 10 | 2.100E+11 | **5.228E-02** | 5.000E+04 | 2.000E+04 | 6.406 |
| $P_1$ | 11 | 2.100E+11 | 4.000E-02 | **3.791E+04** | 2.000E+04 | 8.644 |
| | 12 | 2.100E+11 | 4.000E-02 | **4.374E+04** | 2.000E+04 | 9.754 |
| | 13 | 2.100E+11 | 4.000E-02 | **4.977E+04** | 2.000E+04 | 10.902 |
| | 14 | 2.100E+11 | 4.000E-02 | **5.664E+04** | 2.000E+04 | 12.209 |
| | 15 | 2.100E+11 | 4.000E-02 | **6.535E+04** | 2.000E+04 | 13.867 |
| $P_2$ | 16 | 2.100E+11 | 4.000E-02 | 5.000E+04 | **1.516E+04** | 10.600 |
| | 17 | 2.100E+11 | 4.000E-02 | 5.000E+04 | **1.750E+04** | 10.767 |
| | 18 | 2.100E+11 | 4.000E-02 | 5.000E+04 | **1.991E+04** | 10.939 |
| | 19 | 2.100E+11 | 4.000E-02 | 5.000E+04 | **2.266E+04** | 11.135 |
| | 20 | 2.100E+11 | 4.000E-02 | 5.000E+04 | **2.614E+04** | 11.384 |
| Mean value | 21 | 2.100E+11 | 4.000E-02 | 5.000E+04 | 2.000E+04 | 10.945 |

Table 11 Integer moments of the horizontal displacement of node 3

| Method | Moments ($u_3$) | | | |
|---|---|---|---|---|
| | 1st | 2nd | 3rd | 4th |
| M-DRM | 11.3646 | 136.3186 | 1726.5786 | 23100.6208 |
| MCS | 11.3662 | 136.3447 | 1726.6984 | 23094.7804 |
| Relative error (%) | 0.01407 | 0.0191427 | 0.00693 | -0.0252888 |

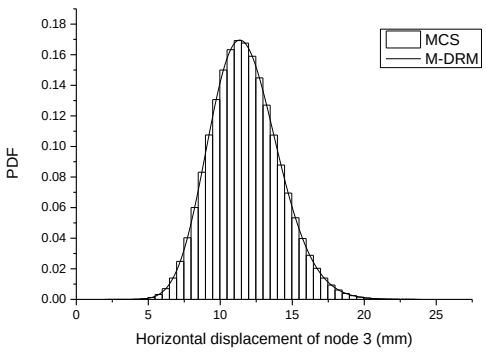


Fig. 5 Distribution of horizontal displacement of node 3

Table 12 Parameters of MaxEnt PDF of horizontal displacement of node 3 derived from M-DRM

| Entropy | $m$ | 0 | 1 | 2 | 3 |
|---|---|---|---|---|---|
| 2.2617 | $\lambda_m$ | 31.5806 | -7.1408 | 1.2744 | -9.5759 |
| | $\alpha_m$ | | 0.5724 | 1.2108 | 0.3959 |
| | $M_Y^{\alpha_m}$ | | 3.994 | 19.10 | 2.601 |

The four integer moments of the horizontal displacement at node 3 ($u_3$) are listed in Table 11. From the Table 11, one can see that the M-DRM method provide highly accurate estimates with relative error less than 0.1%.

The MaxEnt PDF of the horizontal displacement at node 3 ($u_3$) estimated from M-DRM is compared with the simulation result from MCS in Fig. 5. Fractional moments and parameters of MaxEnt distribution are listed in Table 12. Calculations of them involved in the M-DRM procedure are based on Table 10.

Considering the critical displacement 0.015 m proposed above and the estimated PDF in Fig. 5, we can obtain the failure probability of the linear frame structure by integration. The probability of failure from M-DRM is compared with the result from MCS in Table 13. From the Table 13, one can see that the result from M-DRM method also agree well with the exact result from MCS method for

Table 13 Results of example 2

| | M-DRM | MCS |
|---|---|---|
| Failure probability | 0.0936 | 0.0948 |
| Relative error(%) | 1.27 | - |

implicit limit state function. The relative error between them is only 1.27%. However, the M-DRM method costs much less calculation time than MCS method. Such phenomena of outperforming the classical Monte Carlo method also has been found in some particular cases (Sobhani and Milev 2017, Kabaivanov 2015).

Since the two examples above show that the M-DRM method is accurate, efficient, and appreciate for both explicit and implicit limit state functions, it can be applied to a much more complicated flutter reliability analysis of a long span suspension bridge.

## 4. Application to a long span suspension bridge

### *4.1 Description of bridge*

The prototype bridge studied here is a suspension bridge with a 1160 m central span length. The bridge span arrangements are (290+1160+402) m. The bridge deck cross section is an aerodynamically shaped closed streamlined steel box girder with 2.8 m high and 34.7 m wide. More specific sizes of the bridge are shown in Fig. 6.

### *4.2 Finite element modeling*

A three-dimensional finite element model of the long span suspension bridge has been established by ANSYS. Three-dimensional beam44 elements were used to model the bridge towers, main girder and bridge piers. The suspenders and cables were modeled by three-dimensional link8 elements. The second load was modeled by the mass21 elements. Only the suspension bridge in construction state is analyzed in this paper since the structure in operation state can be analyzed with the same method. Table 14 shows the main parameters of streamlined steel box girder of suspension bridge in construction state.

The flutter derivatives were obtained from CFD. The detailed calculation procedure of flutter derivatives is omitted here owing to space reasons For the sake of simplicity, only the flutter derivatives of main girder in construction state at the wind attack angle of 0 degree are considered in the following analyses.

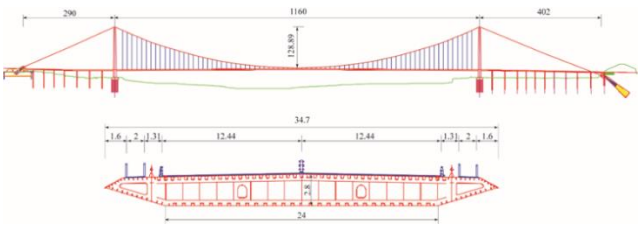


Fig. 6 Arrangement of the bridge span and the bridge deck cross section (unit: m)

Table 14 Main parameters of streamlined steel box girder of suspension bridge in construction state

| Torsional fundamental frequency (Hz) | Vertical fundamental frequency (Hz) | Generalized mass (kg/m) | Generalized mass moment of inertia (kg · m$^2$/m) |
|---|---|---|---|
| 0.3594 | 0.1686 | 14215 | 1372840 |

### *4.3 Deterministic flutter analysis*

In the classical flutter theory, flutter is a divergent self-excited vibration with the interaction of wind and structure. Long span bridges are long and slender structures whose geometric scales tend to be large in one direction and small in the other two directions. The effect of wind on the structure can be expressed in terms of strip theory. Therefore, the two-dimensional (2D) frequency domain analysis theory is a common research method in bridge flutter analysis.

Only first vertical modal and first torsional modal are considered, then the 2D flutter equation can be written as

$$\begin{cases} m\left(\ddot{h}+2\xi_h\omega_h\dot{h}+\omega_h^2 h\right)=L \\ I\left(\ddot{\alpha}+2\xi_\alpha\omega_\alpha\dot{\alpha}+\omega_\alpha^2\alpha\right)=M \end{cases} \tag{26}$$

Where $m$ and $I$ are mass and mass moment of inertia per unit length; $h$ and $\alpha$ are vertical displacement and torsional displacement, respectively; $\omega_h, \omega_\alpha$ are vertical and torsional fundamental frequency, respectively; $\xi_h, \xi_\alpha$ are vertical and torsional damping ratios, respectively; $L$ and $M$ are aerodynamic self-excited forces per unit length.

According to the Scanlan' theory, the 2D aerodynamic self-excited forces can be expressed as

$$\begin{cases} L=\frac{1}{2}\rho U^2(2B)(KH_1^*\frac{\dot{h}}{U}+KH_2^*\frac{B\dot{\alpha}}{U}+K^2H_3^*\alpha+K^2H_4^*\frac{h}{B}) \\ M=\frac{1}{2}\rho U^2(2B^2)(KA_1^*\frac{\dot{h}}{U}+KA_2^*\frac{B\dot{\alpha}}{U}+K^2A_3^*\alpha+K^2A_4^*\frac{h}{B}) \end{cases} \tag{27}$$

Where $\rho$ is air density; $U$ is average wind speed; $B$ is bridge deck width; $h$, $\alpha$ are vertical displacement and torsional displacement, respectively; $K$ is reduced frequency i.e. $K=\frac{B\omega}{U}$; $H_i^*$, $A_i^*$ ($i$=1,2,3,4) are flutter derivatives.

According to the basic theory above, the 2D frequency domain flutter analysis can be achieved by self-edited program based on MATLAB. We call this finite element method. For comparison, both finite element method and empirical formula are used to analyze the flutter response of suspension bridge here. The empirical formula is expressed as: (Cheng *et al*. 2005)

$$V_{cr}=\eta_s\left[1+(\varepsilon-0.5)\sqrt{0.72\mu(\frac{r}{b})}\right]\cdot\omega_h\cdot b \tag{28}$$

Table 15 Comparison between the results obtained by finite element method and by empirical formulas

| Critical flutter velocity | Finite element method | Empirical formulas |
|---|---|---|
| $V_{cr}$ | 66.3(m/s) | 59.8(m/s) |

$$\mu = \frac{m}{\pi \rho b^2} \tag{29}$$

Where $V_{cr}$ is critical flutter velocity, $\eta_s$ is shape coefficient of bridge deck cross section, $\varepsilon$ is frequency ratio between fundamental torsional and bending modes, $r$ is radius of gyration of bridge deck cross section, m is mass per unit length of structure, $\rho$ is air density, b is half width of bridge, $\omega_h$ is circular frequency of the first bending mode.

A comparison of critical flutter velocity between finite element method and empirical formula is shown in Table 15. The result obtained by empirical formula is reasonably close to that by finite element method. Also, the result by empirical formula tend to be conservative. So it can meet the needs of preliminary deterministic analysis of flutter response. However, the difference between finite element method and empirical formula may be magnified in terms of reliability analysis.

### *4.4 Non-deterministic flutter analysis*

As is well known, the structure parameters such as damping ratios, geometric parameters and material properties of the suspension bridge cannot be exactly equal to design values during the process of erection of the bridge. In other words, they may fluctuate in the vicinity of the nominal values. Therefore, structure parameters should be treated as random instead of deterministic variables. Besides, flutter derivatives and extreme wind velocity at the bridge site are also random variables due to experimental or numerical calculation error and wind characteristics. All statistics of these input random variables are shown in Table 16.

The objective of this study is to propose an efficient and accurate method for complicated flutter reliability analysis of suspension bridges which includes of many uncertainties mentioned above. On the other hand, it is very difficult to determine the interrelation of the random variables. For the sake of simplicity, we assume that all these input random variables here are treated as independent from each other.

The reliability of a system is always studied based on a limit state function. In previous studies, most limit state functions for flutter reliability analysis are explicit. And the explicit limit state function for flutter reliability analysis can be estimated by empirical formula which makes critical flutter velocity easy and simple to be solved.

However, some parameters such as damping ratio and structural properties cannot be directly considered in explicit limit state function. This may lead to greater error in process of reliability analysis.

Table 16 Random variables for flutter reliability analysis of suspension bridge

| Variable | Description | distribution | units | mean | cov | Reference |
|---|---|---|---|---|---|---|
| $X_1$ | Mass per unit length | Normal | Kg | 14215 | 0.1 | Assumed |
| $X_2$ | Mass moment of inertia per unit length | Normal | Kg·m$^2$ | 1372840 | 0.1 | Assumed |
| $X_3$ | Elastic modulus | Normal | - | $2.1\times10^{11}$ | 0.1 | Assumed |
| $X_4$ | Cross sectional area | Normal | m$^2$ | 1.555 | 0.1 | Assumed |
| $X_5$ | Sectional moments of inertia | Normal | m$^4$ | 2.045 | 0.1 | Assumed |
| $X_6$ | | Normal | m$^4$ | 153.493 | 0.1 | Assumed |
| $X_7$ | | Normal | m$^4$ | 6.05 | 0.1 | Assumed |
| $X_8$ | Damping ratio | Lognormal | - | 0.005 | 0.4 | Pourzeynail and Datta 2002 |
| $X_9$ | Basic wind velocity | Type I | m/s | 27.20 | 0.15 | Xu *et al*. 2006 |
| $X_{10}$ | Gust speed factor | Normal | - | 1.24 | 0.07 | Ge *et al*. 2000 |
| $X_{11}$ | Flutter derivatives parameter | Lognormal | - | 1 | 0.2 | Pourzeynail and Datta 2002 |

For the sake of simplicity, a parameter $X_{11}$ is introduced to consider the uncertainties arising from the insufficient knowledge of flutter derivatives. The implicit limit state function can be expressed as

$$R = \frac{X_{11} \cdot V_{cr}(X_1, X_2, X_3, X_4, X_5, X_6, X_7, X_8)}{X_9 \cdot X_{10}} \tag{30}$$

Such that the probability of failure can be computed as $P_F = P_r[R \le 1.0]$

The flutter reliability analysis of suspension bridge can be conducted by the same solution procedures of two examples proposed above. The numerical integration grid of flutter reliability analysis is reported in Table 17. And the parameters of MaxEnt PDF of limit state function $R$ derived from M-DRM are listed in Table 18. Thus, we can get the estimated PDF of $R$ which is shown in Fig. 7. It can be used to calculate the failure probability of flutter.

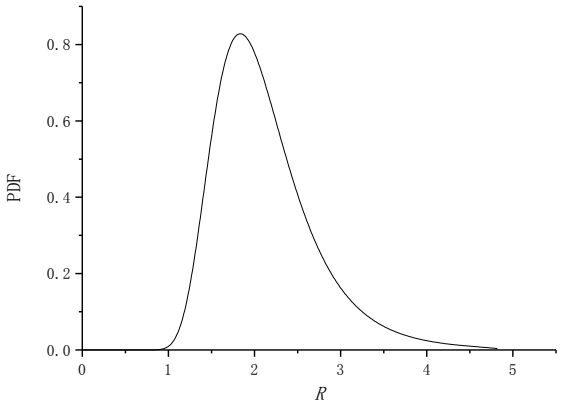


Fig. 7 Distribution of limit state function R

Table 17 Numerical integration grid for computing the moments with M-DRM: suspension bridge

| Variable | NO. | Numerical integration grid | | | | *R* |
|---|---|---|---|---|---|---|
| | | $X_1$(Kg) | $X_2$(Kg·m$^2$) | $X_{10}$ | $X_{11}$ | |
| $X_1$ | 1 | **1.015E+04** | 1.373E+06 | 1.240 | 1 | 1.823 |
| | 2 | **1.229E+04** | 1.373E+06 | 1.240 | 1 | 1.903 |
| | 3 | **1.422E+04** | 1.373E+06 | 1.240 | 1 | 1.966 |
| | 4 | **1.614E+04** | 1.373E+06 | 1.240 | 1 | 2.016 |
| | 5 | **1.828E+04** | 1.373E+06 | 1.240 | 1 | 2.064 |
| $X_2$ | 6 | 1.422E+04 | **9.806E+05** | 1.240 | 1 | 1.782 |
| | 7 | 1.422E+04 | **1.187E+06** | 1.240 | 1 | 1.886 |
| | 8 | 1.422E+04 | **1.373E+06** | 1.240 | 1 | 1.966 |
| | 9 | 1.422E+04 | **1.559E+06** | 1.240 | 1 | 2.034 |
| | 10 | 1.422E+04 | **1.765E+06** | 1.240 | 1 | 2.099 |
| | ⋮ | ⋮ | ⋮ | ... ⋮ | ⋮ | ⋮ |
| $X_{10}$ | 46 | 1.422E+04 | 1.373E+06 | **0.991** | 1 | 2.459 |
| | 47 | 1.422E+04 | 1.373E+06 | **1.122** | 1 | 2.172 |
| | 48 | 1.422E+04 | 1.373E+06 | **1.240** | 1 | 1.966 |
| | 49 | 1.422E+04 | 1.373E+06 | **1.358** | 1 | 1.795 |
| | 50 | 1.422E+04 | 1.373E+06 | **1.489** | 1 | 1.637 |
| $X_{11}$ | 51 | 1.422E+04 | 1.373E+06 | 1.240 | **0.584** | 1.148 |
| | 52 | 1.422E+04 | 1.373E+06 | 1.240 | **0.768** | 1.510 |
| | 53 | 1.422E+04 | 1.373E+06 | 1.240 | **0.984** | 1.933 |
| | 54 | 1.422E+04 | 1.373E+06 | 1.240 | **1.259** | 2.475 |
| | 55 | 1.422E+04 | 1.373E+06 | 1.240 | **1.656** | 3.255 |
| Mean value | 56 | 1.422E+04 | 1.373E+06 | 1.240 | 1 | 1.966 |

Table 18 Parameters of MaxEnt PDF of R derived from M-DRM

| Entropy | *m* | 0 | 1 | 2 | 3 |
|---|---|---|---|---|---|
| 0.7473 | $\lambda_m$ | 32.7713 | 31.1664 | -61.5712 | 6.8906 |
| | $\alpha_m$ | | -1.3567 | -0.4203 | -2.4513 |
| | $M_Y^{\alpha_m}$ | | 0.4576 | 0.7771 | 0.2606 |

Table 19 Comparison of results for various methods

| Method | Method I | Method II |
|---|---|---|
| $P_f$ | 5.24e-4 | 0.00244 |

Two methods are used to calculate the failure probability of flutter of suspension bridge here. Method I is finite element method based on M-DRM; Method II is empirical formula based on MCS with $10^6$ samples. The results are given in Table 19. From the Table 19, one can see that: (1) although the deterministic critical flutter velocities calculated by Method I and Method II are reasonably close (see Table 15), there are also significant differences in the failure probability of flutter (about 4.65 times) between the two. This is because that the error existed in the two is magnified in process of flutter reliability analysis. Also, the numbers of system uncertainties considered in Method II are less than Method I. On the other hand, the result by Method II is only a too conservative estimate for flutter reliability analysis but is not accurate adequately. So Method II is not suitable for reliability analysis of bridge flutter. (2) Method I has higher computational efficiency than Method II for complicated flutter reliability analysis since method I is only based on the 56 (=1+11×5) deterministic model evaluations instead of $10^6$ samples.

## 5. Conclusions

A reliability analysis method has been proposed based on the maximum entropy principle in which constraints are specified in terms of fractional moments in this paper. The fractional moments involved in the MaxEnt procedure are much more effective in modeling the distribution tail than the integer moments.

Two examples have been presented to illustrate the numerical effective and accuracy of M-DRM method proposed in this paper. Compared with FORM and SORM methods, the M-DRM method is appreciate for both explicit and implicit limit state functions and has more higher numerical accuracy; Compared with MCS with $10^6$ samples, the M-DRM method has the advantage of the high computational efficiency which is considerable improved by using the Gaussian quadrature for low dimensional integration. For most examples, highly accurate results only need a few deterministic model evaluations. Finally, the M-DRM is used to analyze the flutter reliability of suspension bridge to verify the result obtained by empirical formula. One can see that empirical formula is not suitable for reliability analysis of bridge flutter.

In summary, the proposed M-DRM and the adopting of fractional moments in this paper provide an alternate and efficient way to analyze a much more complicated flutter reliability of long span suspension bridge. Furthermore, wider application of the proposed method in other fields is being explored.

## Acknowledgments

The research described in this paper was financially supported by the Natural Science Foundation of China under grant number 51378443 and U1434205.. This support is much appreciated. The valuable comments of the anonymous reviewers of the paper are also acknowledged.

## References

Agar, T.J.A. (1988), "The analysis of aerodynamic flutter of suspension bridges", *Comput . Struct.*, **30**(3), 593-600.

Balomenos, G. (2015), "Probabilistic finite element analysis of structures using the multiplicative dimensional reduction method", Ph.D. Dissertation, University of Waterloo, Waterloo, Canada.

Balomenos, G.P., Genikomsou, A.S., Polak, M.A. and Pandey, M.D. (2015), "Efficient method for probabilistic finite element analysis with application to reinforced concrete slabs", *Eng. Struct.*, **103**, 85-101.

Bucher, C.G. and Bourgund, U. (1990), "A fast and efficient response surface approach for structural reliability problems", *Struct. Saf.*, **7**(1), 57-66.

Cheng, J., Cai, C.S., Xiao, R.C. and Chen, S.R. (2005), "Flutter reliability analysis of suspension bridges", *J. Wind Eng. Ind. Aerod.*, **93**(10), 757-775.

Chen, S.R. and Cai, C.S. (2003), "Evolution of long-span bridge response to wind-numerical simulation and discussion", *Comput. Struct.*, **81**(21), 2055-2066.

Davis, P.J. and Rabinowitz, P. (1984), Methods of Numerical Integration, Academic Press Inc., London, UK.

Faravelli, L. (1989), "Response-surface approach for reliability analysis", *J. Eng. Mech.*, **115**(12), 2763-2781.

Ge, Y.J., Xiang, H.F. and Tanaka, H. (2000), "Application of a reliability analysis model to bridge flutter under extreme winds", *J. Wind Eng. Ind. Aerod.*, **86**(2), 155-167.

Gzyl, H., Milev, M. and Tagliani, A. (2007). "Discontinuous payoff option pricing by Mellin transform: A probabilistic approach", *Finance Res. Lett.*, **20**, 281-288.

Han, Y., Liu, S. and Cai, C.S. (2015), "Flutter stability of a long-span suspension bridge during erection", *Wind Struct.*, **21**(1), 41-61.

Hong, Y., Lee, S. and Li, T. (2015). "Numerical method of pricing discretely monitored Barrier option", *J. Comput. Appl. Math.*, **278**, 149-161.

Huh, J. and Haldar, A. (2001), "Stochastic finite-element-based seismic risk of nonlinear structures", *J. Struct. Eng.*, **127**(3), 323-329.

Huh, J. and Haldar, A. (2002), "Seismic reliability of non-linear frames with PR connections using systematic RSM", *Probab. Eng. Mech.*, **17**(2), 177-190.

Inverardi, P.N., Petri, A., Pontuale, G. and Tagliani, A. (2005), "Stieltjes moment problem via fractional moments", *Appl. Math. Comput.*, **166**(3), 664-677.

Jaynes, E.T. (1957), "Information theory and statistical mechanics", *Phys. Rev.*, **108**(2), 171-190.

Kabaivanov, S., Malechkova, A., Marchev, A., Milev, M., Markovska, V. and Nikolova, K. (2015), "A step beyond the Monte Carlo method in economics: Application of multivariate normal distribution", **1690**(1), 227-240.

Kaymaz, I. and McMahon, C.A. (2005), "A response surface method based on weighted regression for structural reliability analysis", *Probab. Eng. Mech.*, **20**(1), 11-17.

Lagarias, J.C., Reeds, J.A., Wright, M.H. and Wright, P.E. (1998), "Convergence properties of the Nelder--Mead simplex method in low dimensions", *SIAM J. Optimiz.*, **9**(1), 112-147.

Larsen, A. (1997), "Prediction of aeroelastic stability of suspension bridges during erection", *J. Wind Eng. Ind. Aerod.*, **72**, 265-274.

Li, G. and Zhang, K. (2011), "A combined reliability analysis approach with dimension reduction method and maximum entropy method", *Struct. Multidiscip.O.*, **43**(1), 121-134.

Li, G., Rosenthal, C. and Rabitz, H. (2001), "High dimensional model representations", *J. Phys. Chem. A*, **105**(33), 7765-7777.

Liu, Y.W. and Moses, F. (1994), "A sequential response surface method and its application in the reliability analysis of aircraft structural systems", *Struct. Saf.*, **16**(1-2), 39-46.

Milev, M., Inverardi, P.N. and Tagliani, A. (2012), "Moment information and entropy evaluation for probability densities", *Appl. Math. Comput.* **218**(9), 5782-5795.

Milev, M. and Tagliani, A. (2017). "Entropy convergence of finite moment approximations in Hamburger and Stieltjes problems", *Stat. Probabil. Lett.*, **120**, 114-117.

Nowak, A.S., Nowak, S. and Szerszen, M.M. (2003), "Calibration of design code for buildings (ACI 318): part 1 - statistical models for resistance", *Am. Concrete Inst. Struct. J.*, **100**, 377-382.

Ostenfeld-Rosenthal, P., Madsen, H.O. and Larsen, A. (1992), "Probabilistic flutter criteria for long span bridges", *J. Wind Eng. Ind. Aerod.*, **42**(1), 1265-1276.

Pandey, M.D. and Zhang, X. (2012), "System reliability analysis of the robotic manipulator with random joint clearances", *Mech. Mach. Theory*, **58**, 137-152.

Pourzeynali, S. and Datta, T.K. (2002), "Reliability analysis of suspension bridges against flutter", *J. Sound Vib.*, **254**(1), 143-162.

Prenninger, P.H.W., Matsumoto, M., Shiraishi, N., Izumi, C. and Tsukiyama, Y. (1990), "Reliability of bridge structures under wind loading: consideration of uncertainties of wind load parameters", *J. Wind Eng. Ind. Aerod.*, **33**(1-2), 385-394.

Rabitz, H. and Aliş, Ö.F. (1999), "General foundations of high-dimensional model representations", *J. Math. Chem..*, **25**(2-3), 197-233.

Rahman, S. and Xu, H. (2004), "A univariate dimension-reduction method for multi-dimensional integration in stochastic mechanics", *Probab. Eng. Mech.*, **19**(4), 393-408.

Rajashekhar, M.R. and Ellingwood, B.R. (1993), "A new look at the response surface approach for reliability analysis", *Struct. Saf.*, **12**(3), 205-220.

Ramírez, P. and Carta, J.A. (2006), "The use of wind probability distributions derived from the maximum entropy principle in the analysis of wind energy", *Energ. Convers. Manage.*, **47**(15), 2564-2577.

Shi, X., Li, J., Xiong, Q., Wu, Y. and Yuan, Y. (2016). "Research of uniformity evaluation model based on entropy clustering in the microwave heating processes", *Neurocomputing*, **173**, 562-572.

Sobhani, A. and Milev, M. (2017). "A Numerical Method for Pricing Discrete Double Barrier option by Legendre Multi-wavelet", *J. Comput. App. Math.*.

Taufer, E., Bose, S. and Tagliani, A. (2009), "Optimal predictive densities and fractional moments", *Appl. Stoch. Model. Bus.*, **25**(1), 57-71.

Xu, F.Y., Chen, A.R. and Zhang, J.R. (2006), "Flutter reliability of cable supported bridge", *China J. Highway Transport*, 19(5), 59-64. In Chinese.

Yao, T.H.J. and Wen, Y.K. (1996), "Response surface method for time-variant reliability analysis", *J. Struct. Eng.*, **122**(2), 193-201.

Zhang, W.M., Ge, Y.J. and Levitan, M.L. (2011), "Aerodynamic flutter analysis of a new suspension bridge with double main spans", *Wind Struct.*, **14**(3), 187-208.

Zhang, X. and Pandey, M.D. (2013), "Structural reliability analysis based on the concepts of entropy, fractional moment and dimensional reduction method", *Struct. Saf.*, **43**, 28-40.

Zhang, X., Pandey, M.D. and Zhang, Y. (2011), "A numerical method for structural uncertainty response computation", *Science China Technol. Sci.*, **54**(12), 3347-3357.

Zheng, Y. and Das, P.K. (2000), "Improved response surface method and its application to stiffened plate reliability analysis", *Eng. Struct.*, **22**(5), 544-551.

Zwillinger, D. (2011), CRC standard mathematical tables and formulae, CRC press, Taylor and Francis Group, Boca Raton, USA.

*CC*